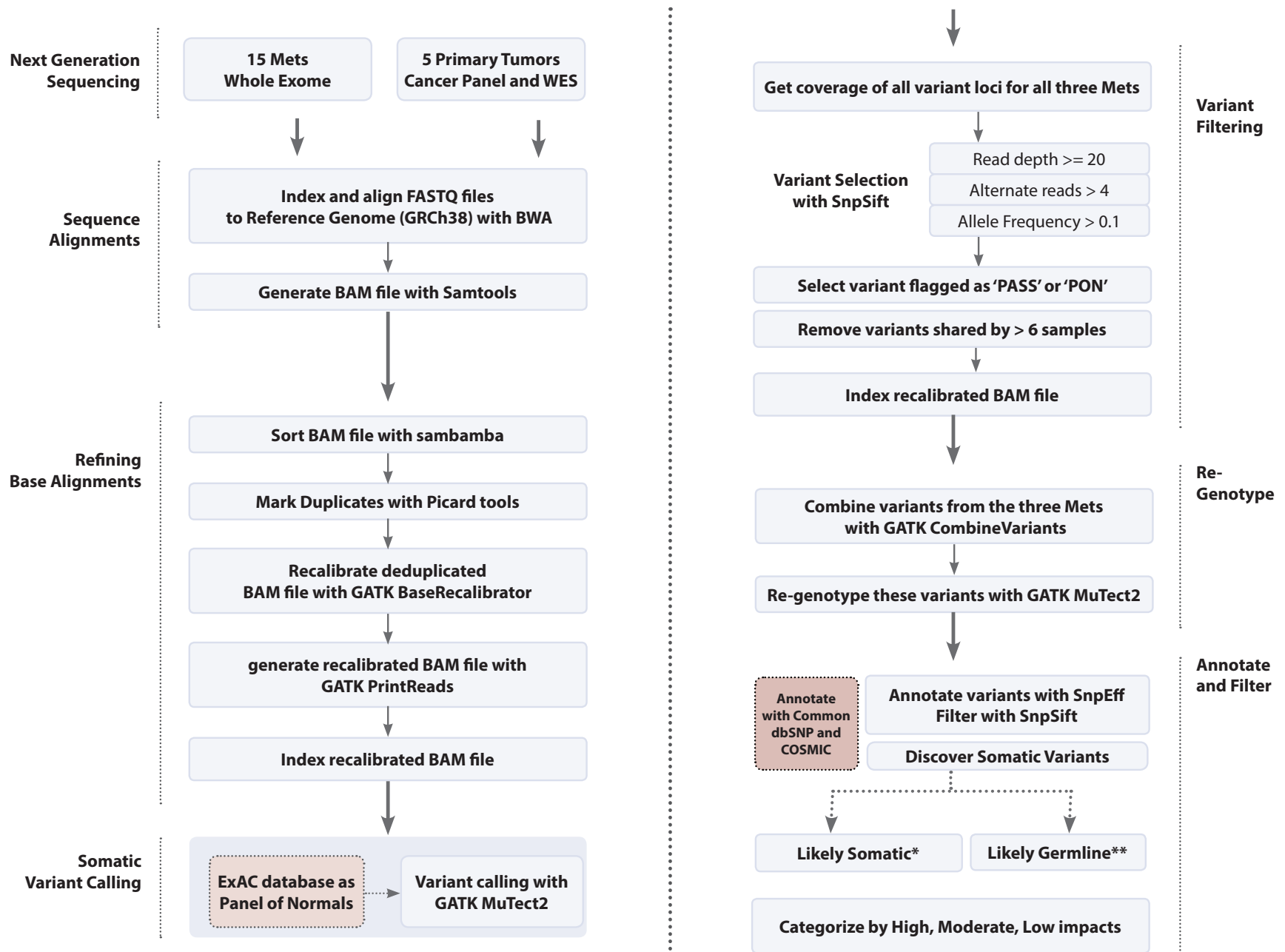
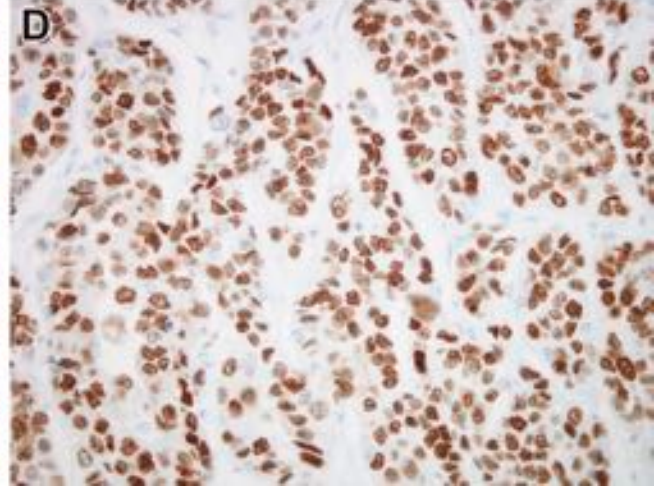
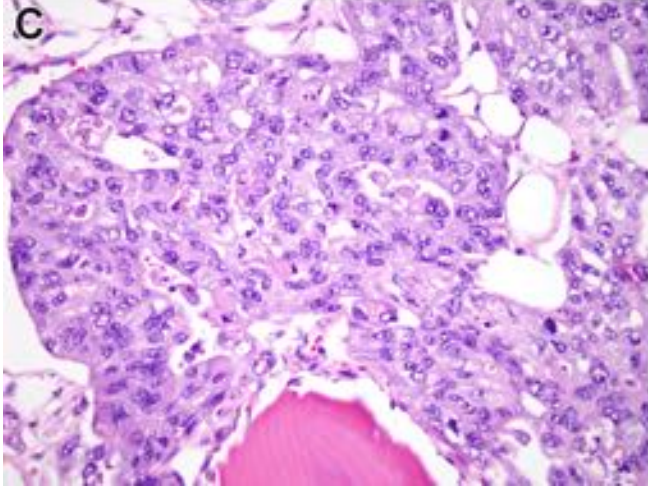
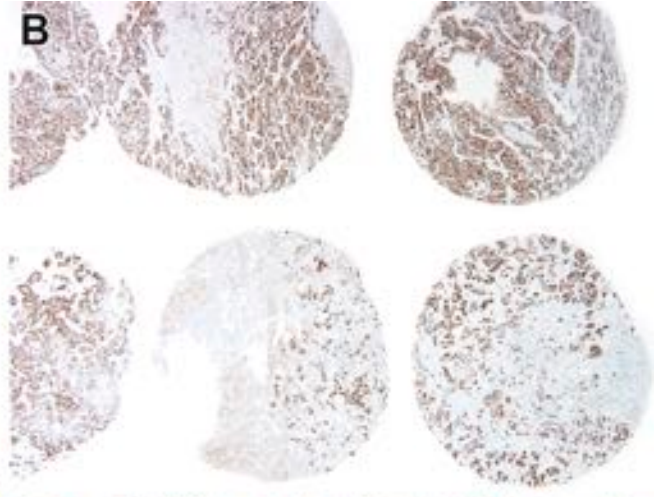
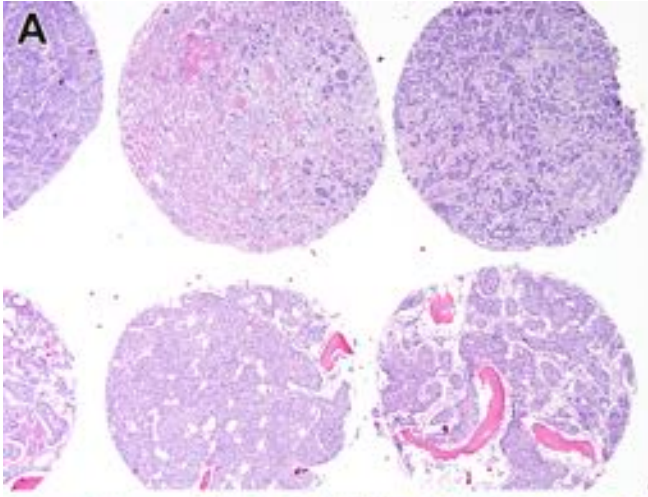


Figure S4



*Variants not in PON or dbSNP

**Variants in PON or Common dbSNP database



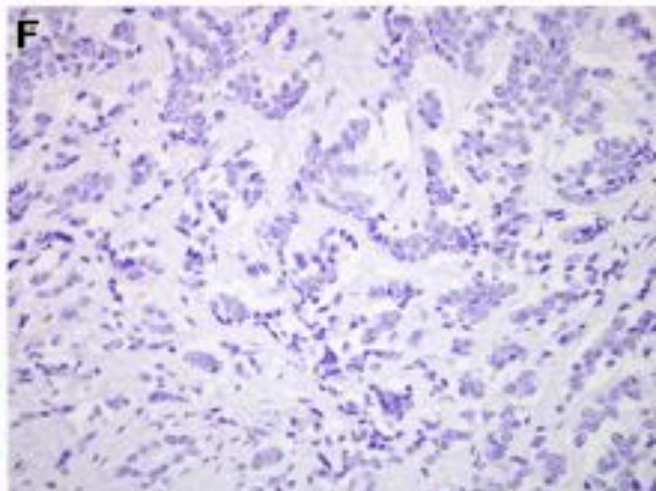
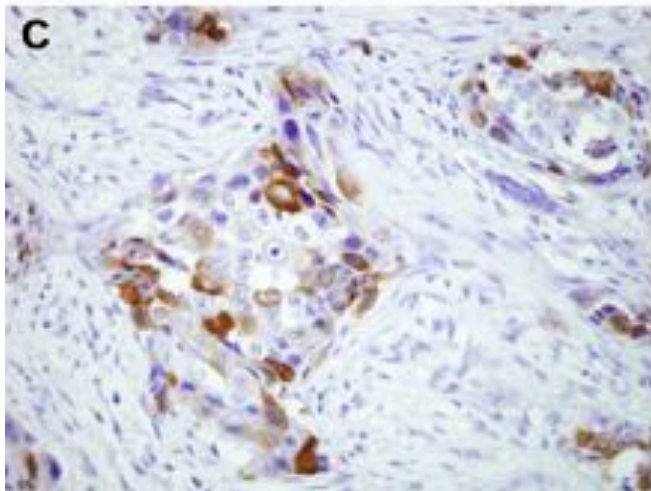
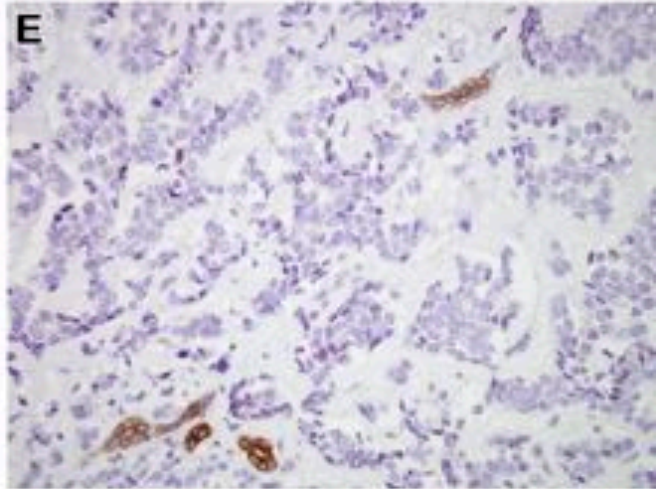
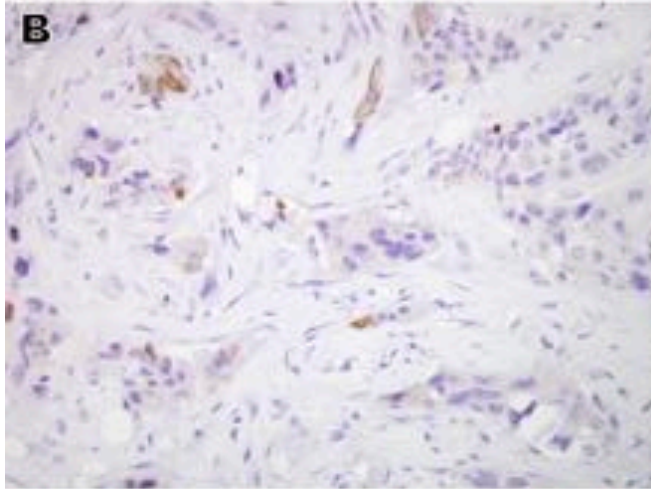
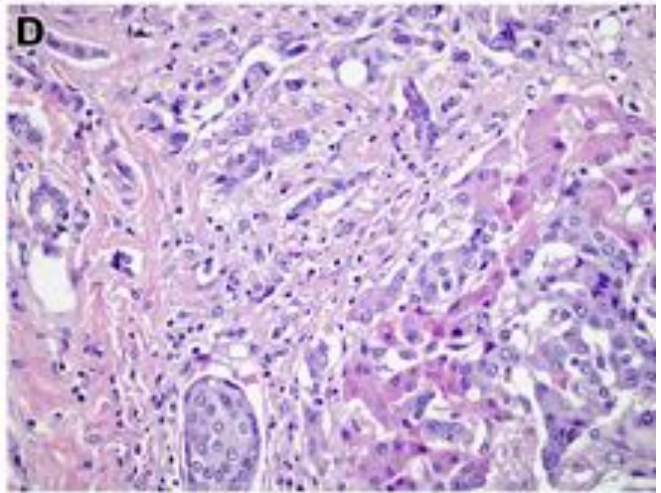
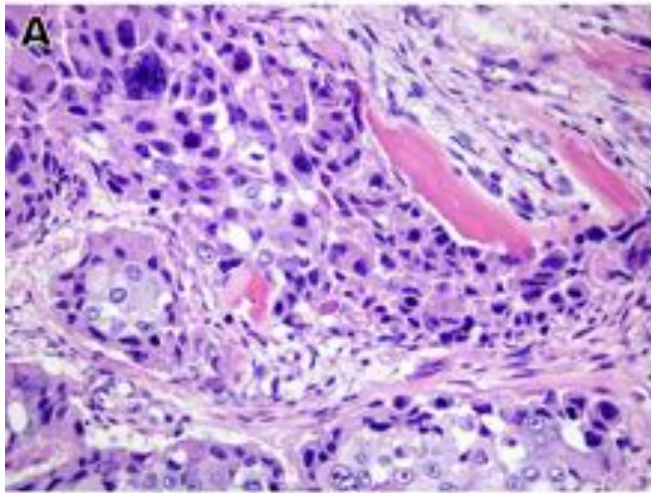


Figure S3

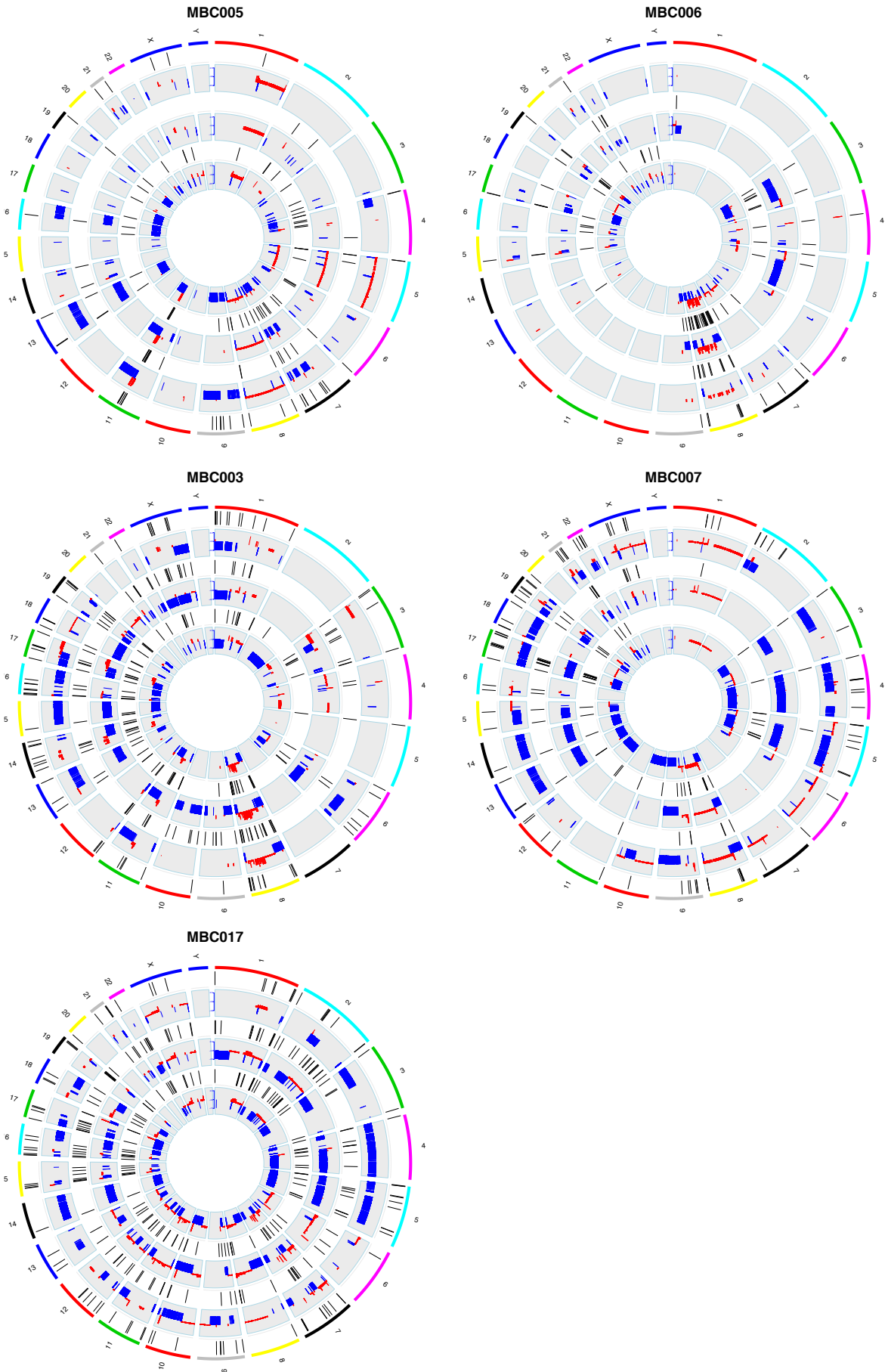
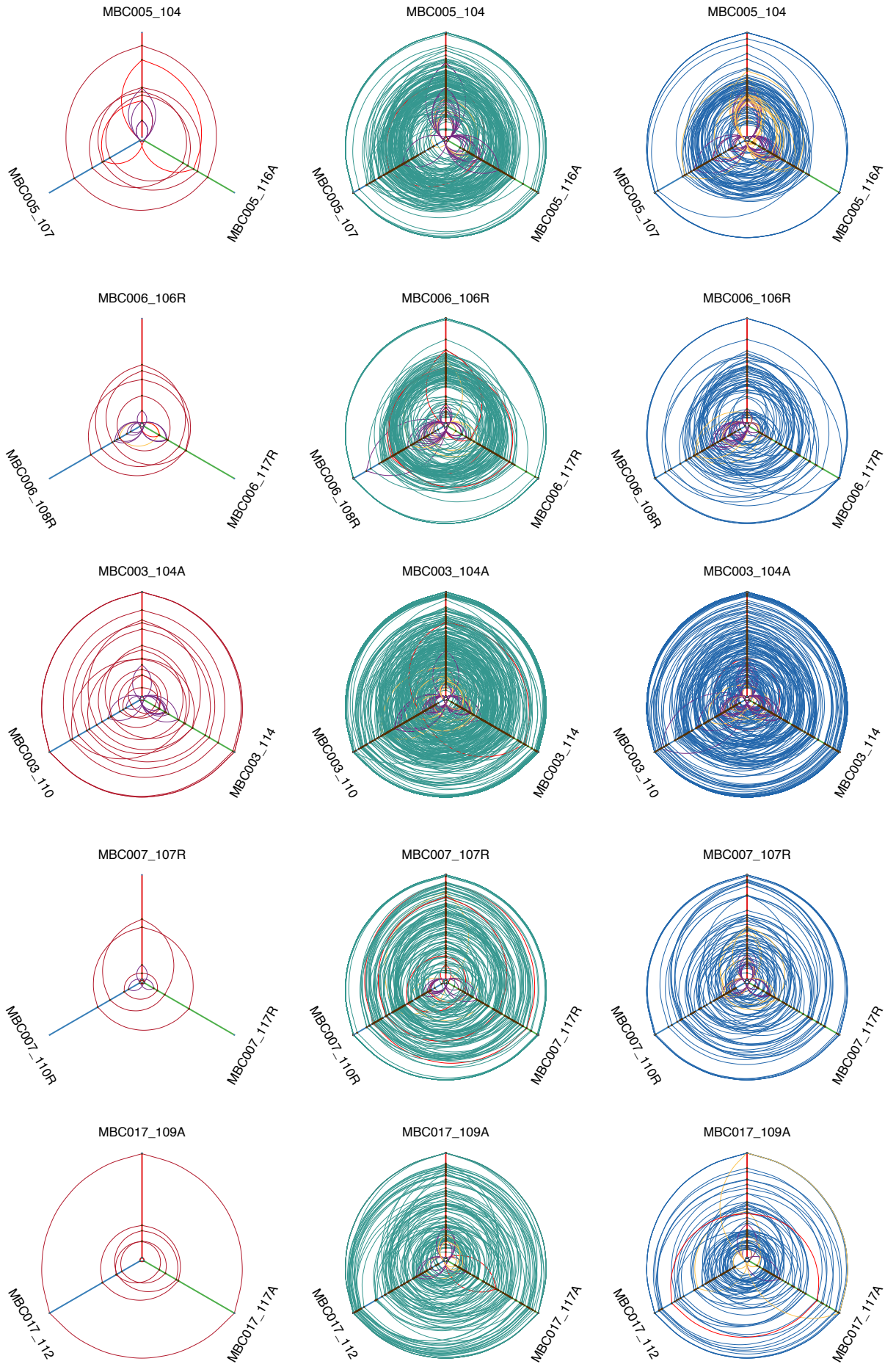
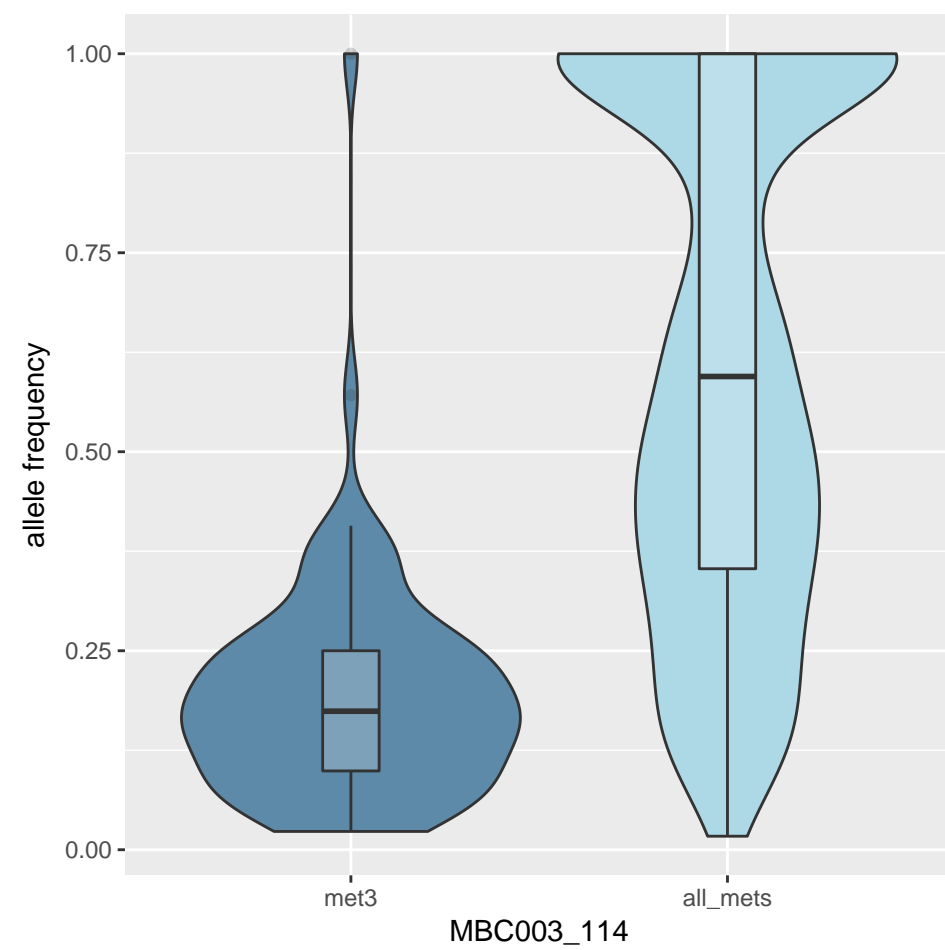
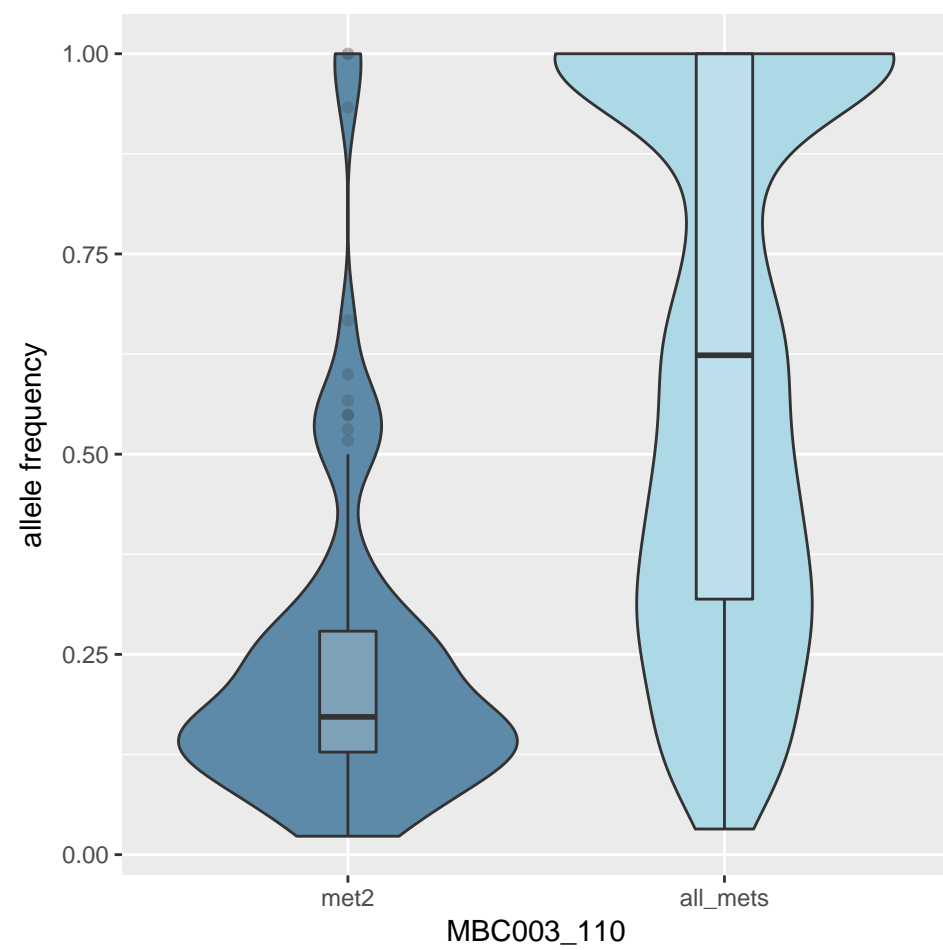
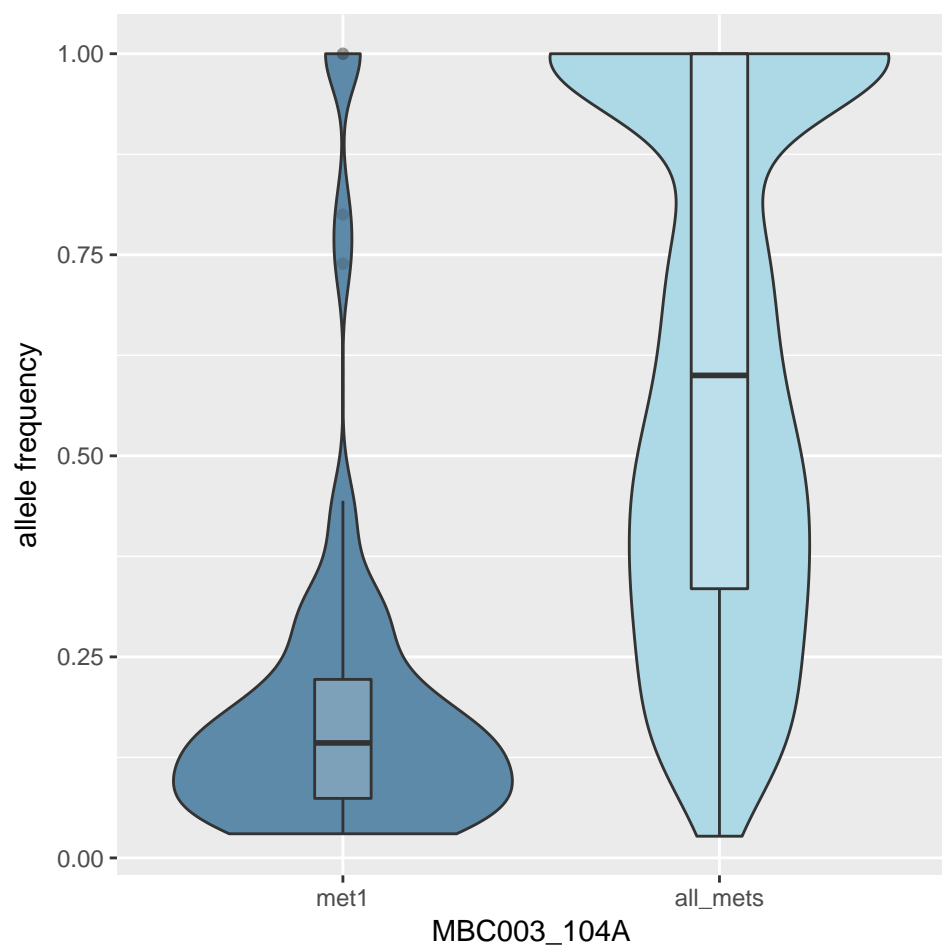
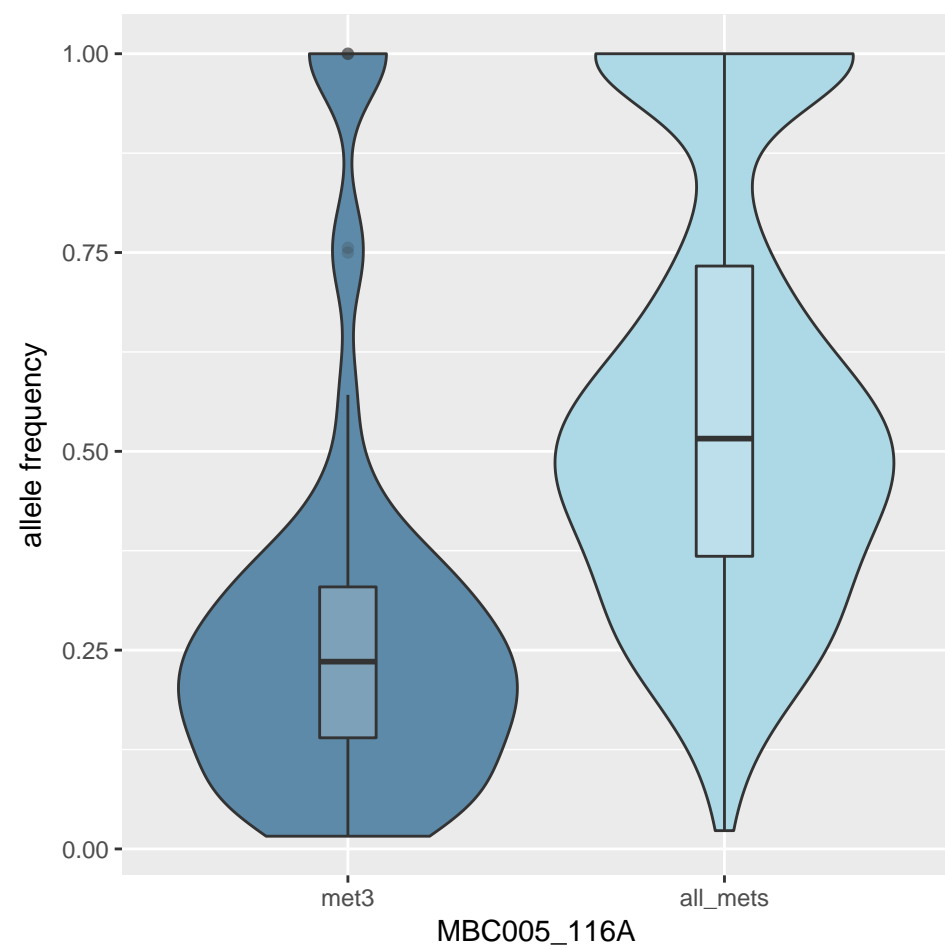
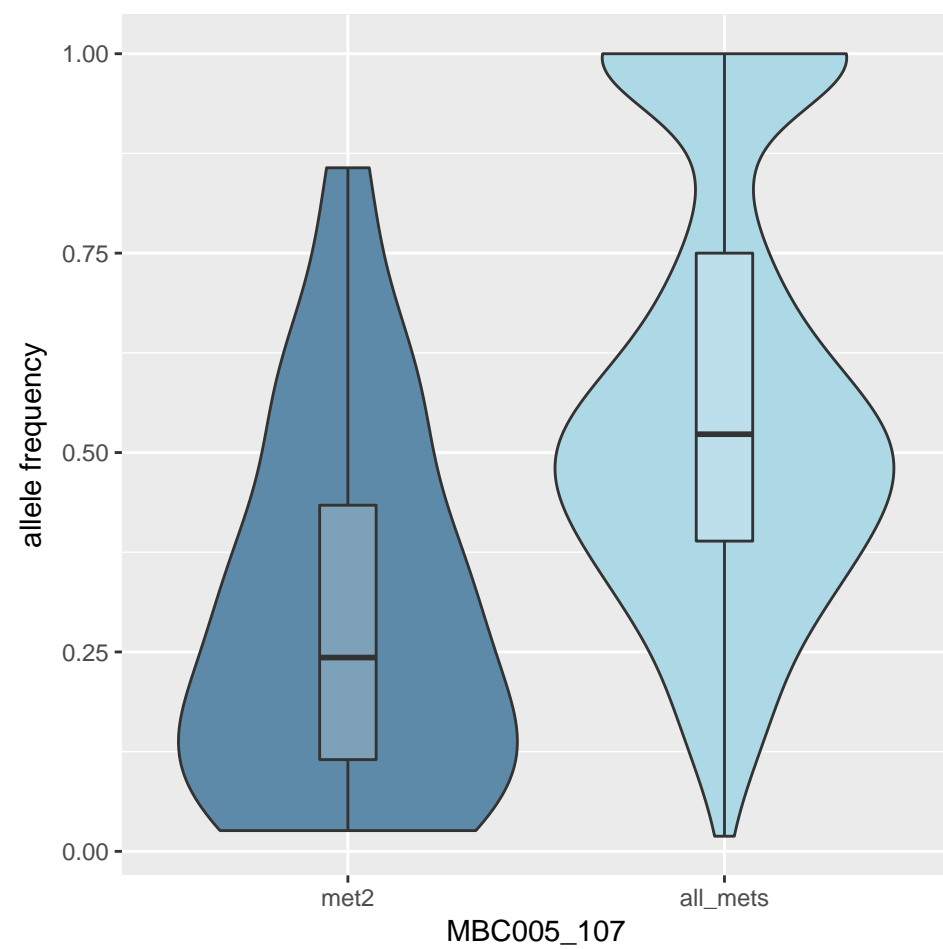
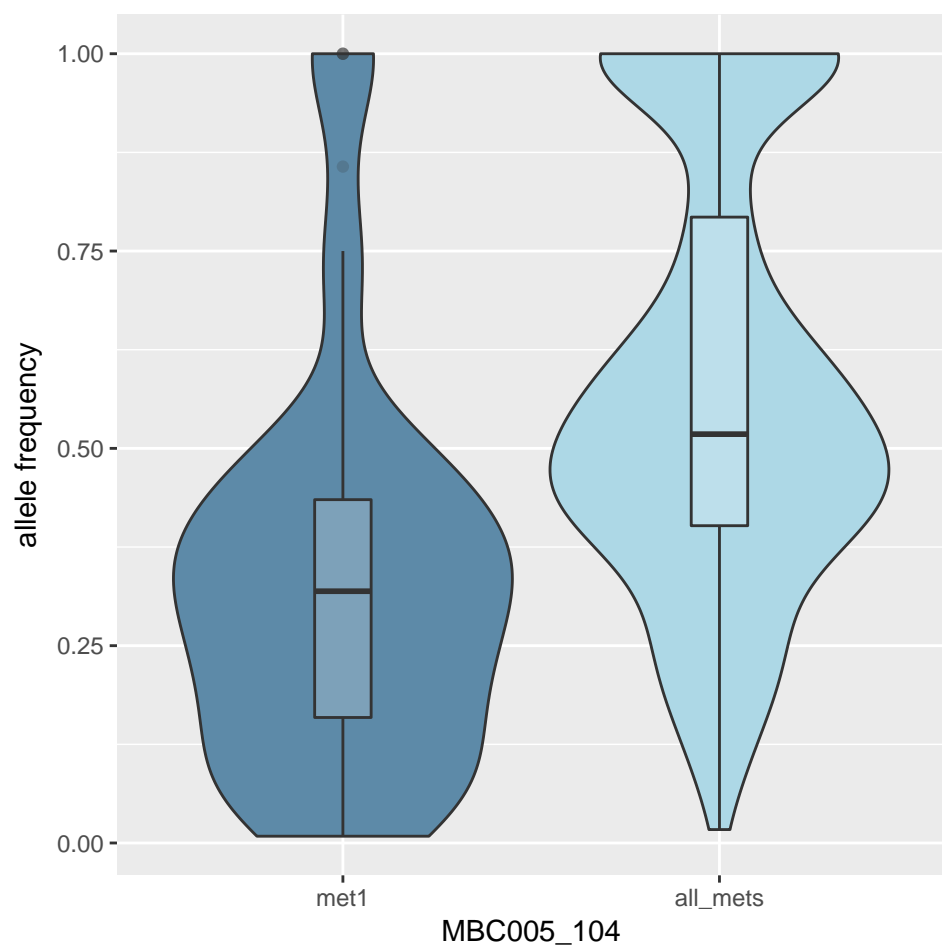
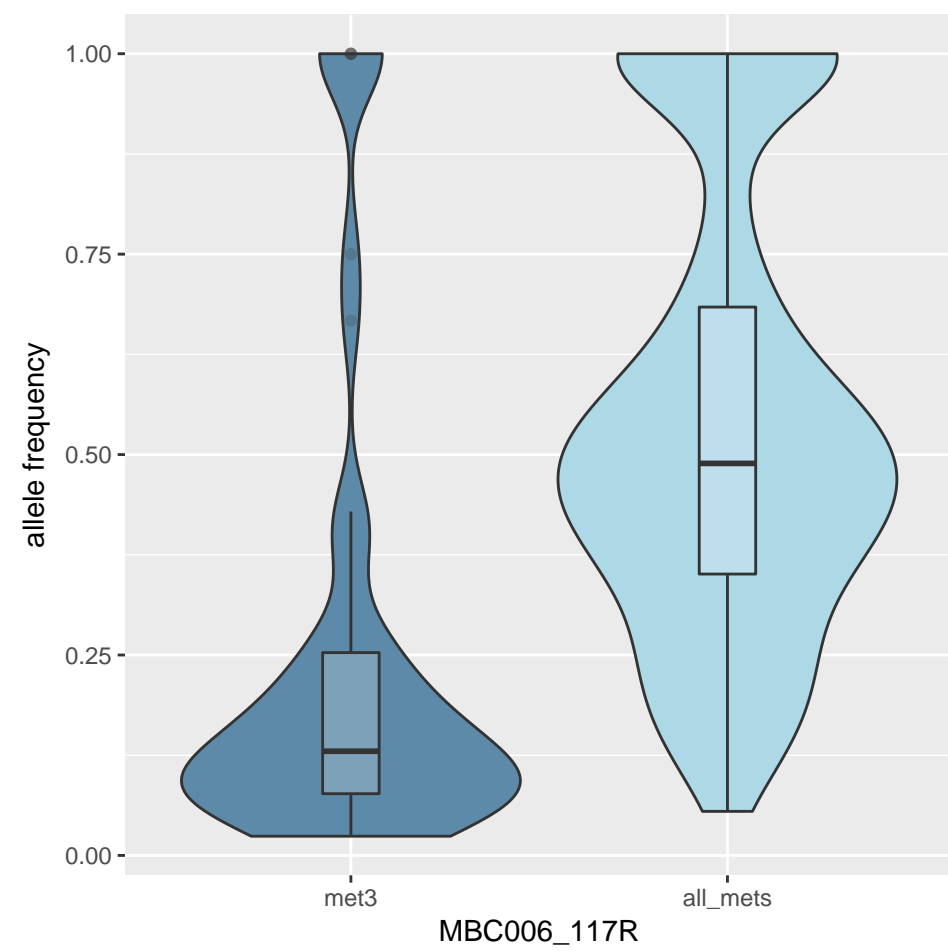
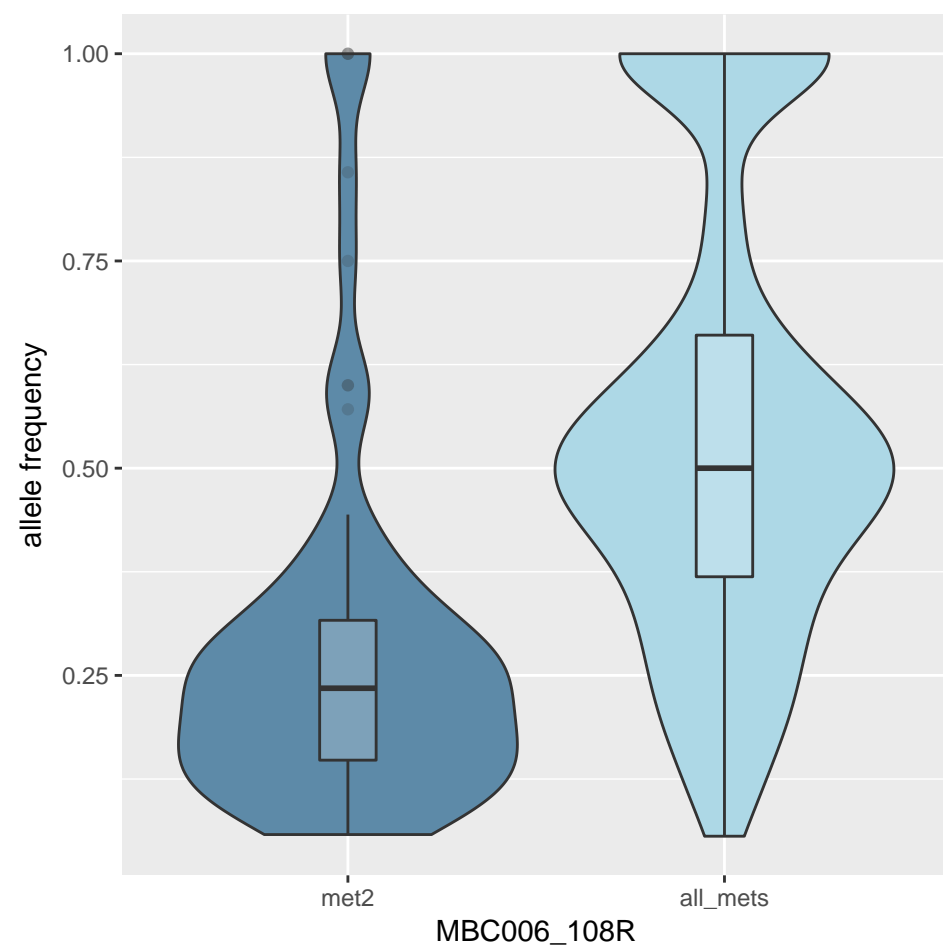
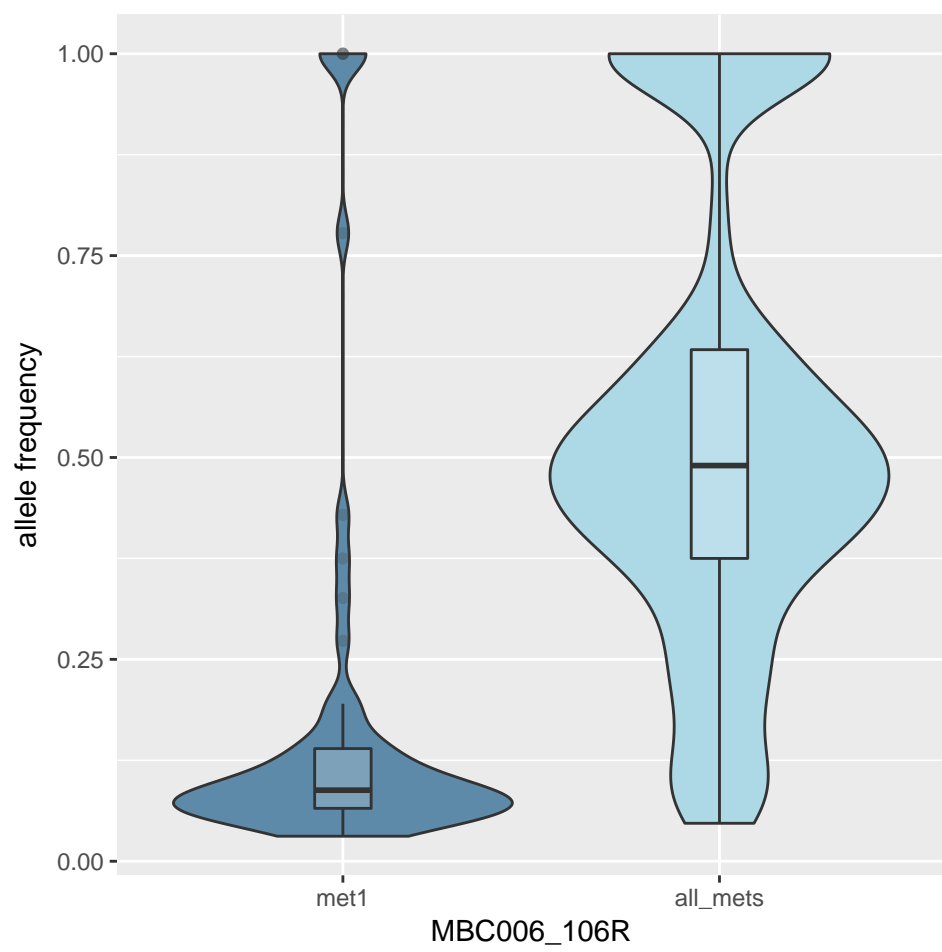


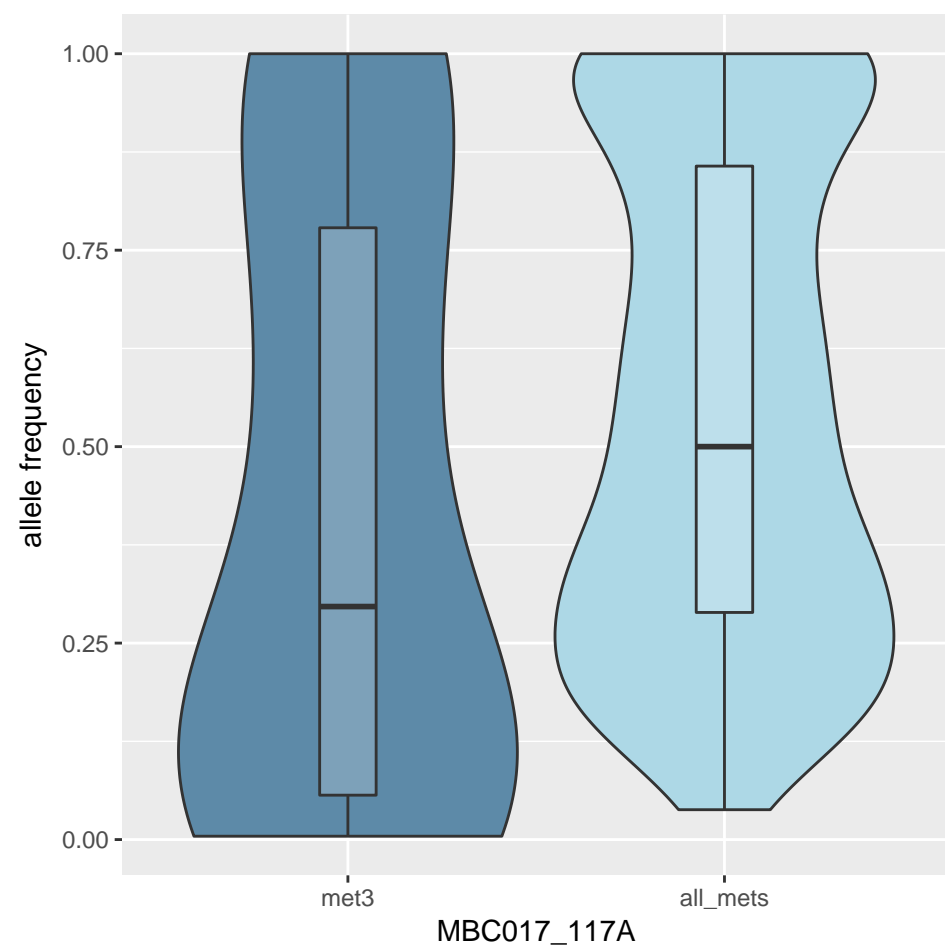
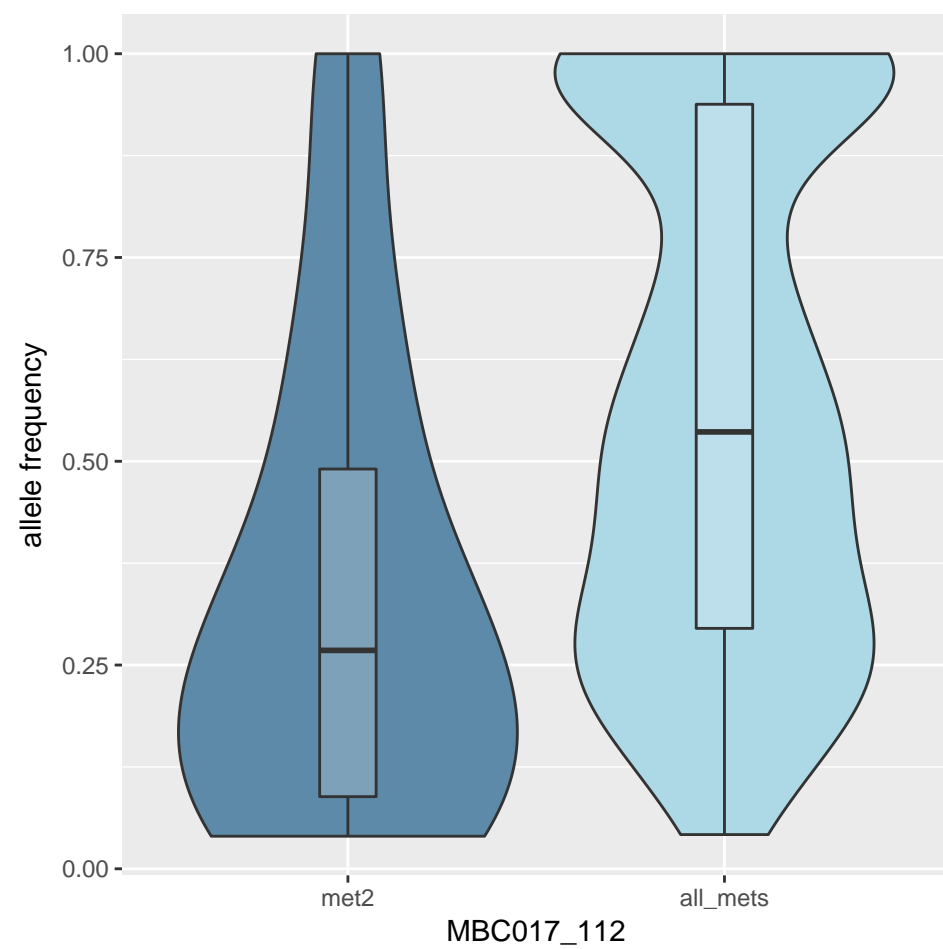
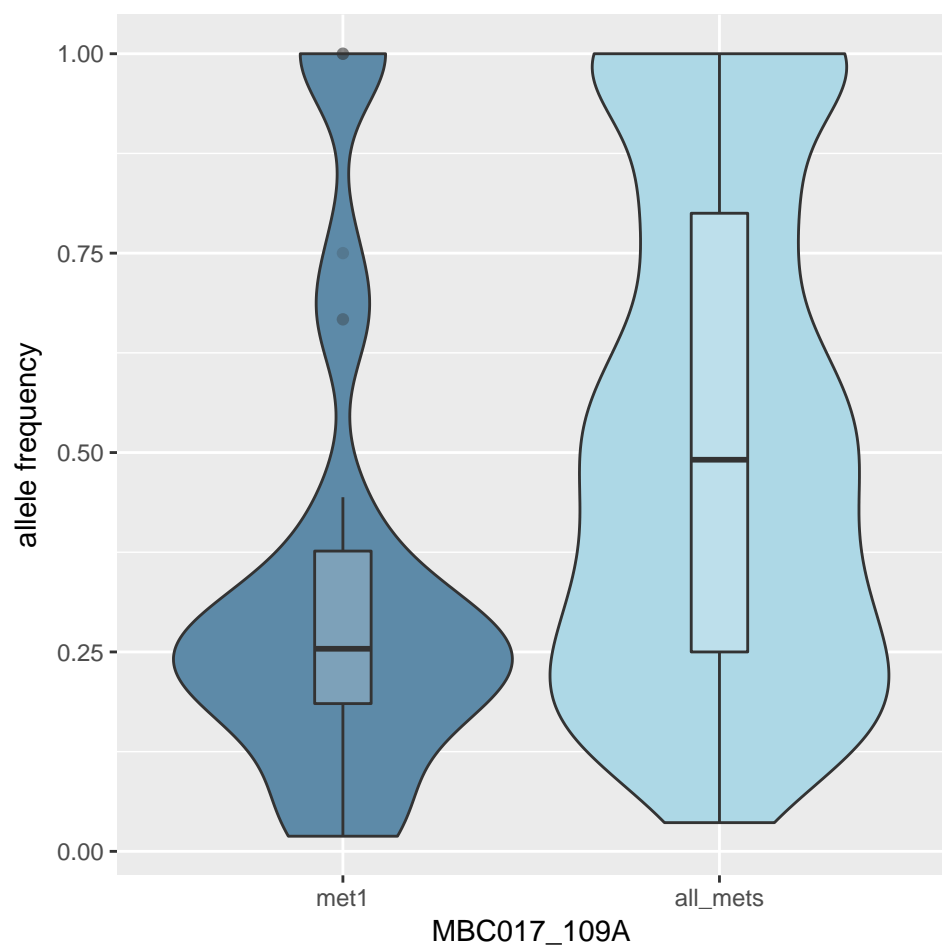
Figure S6

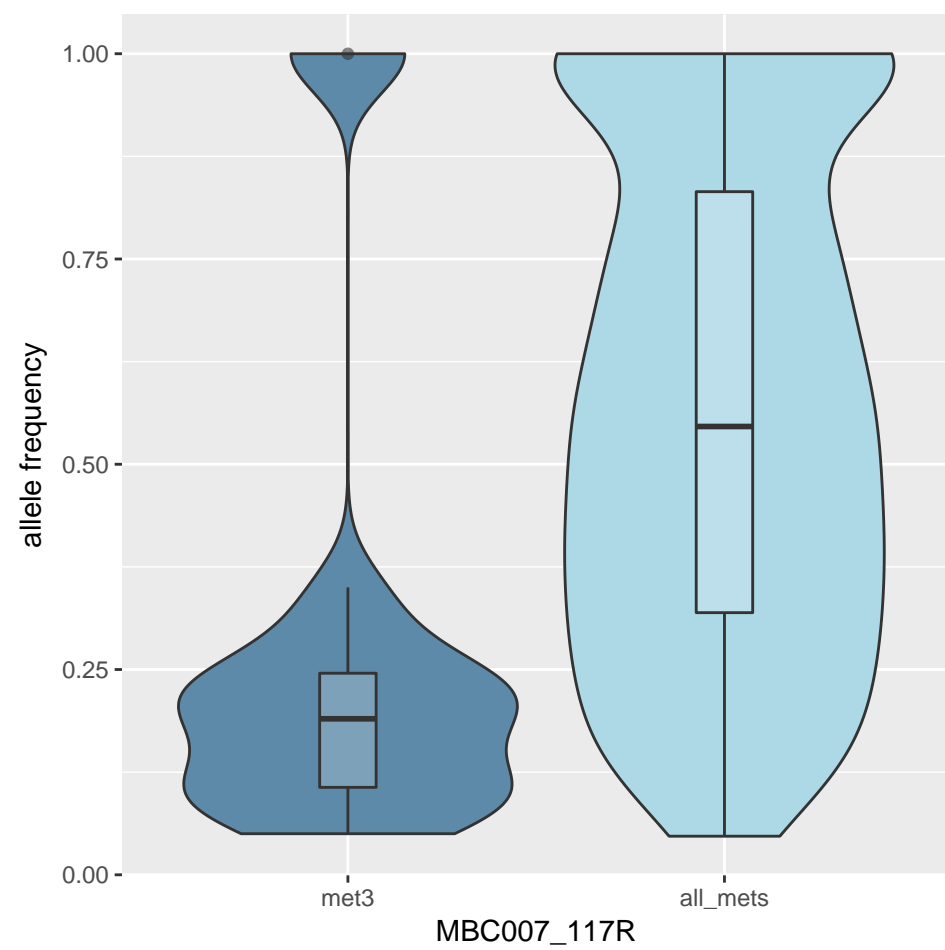
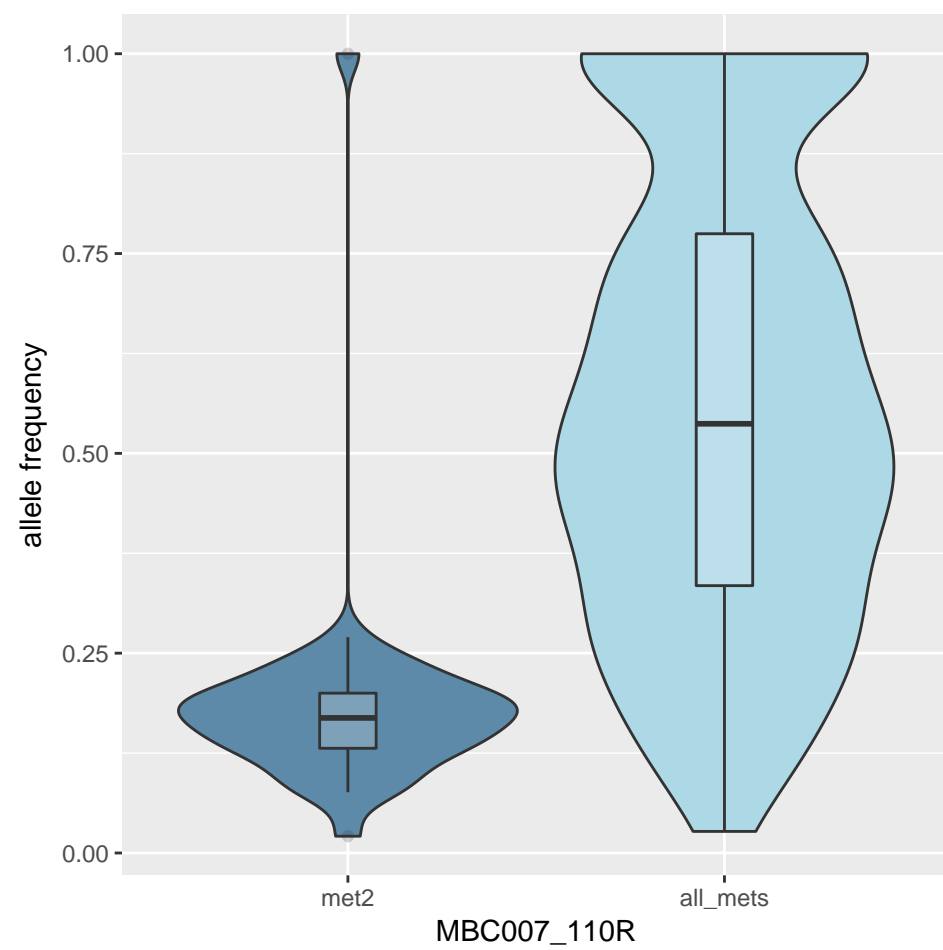
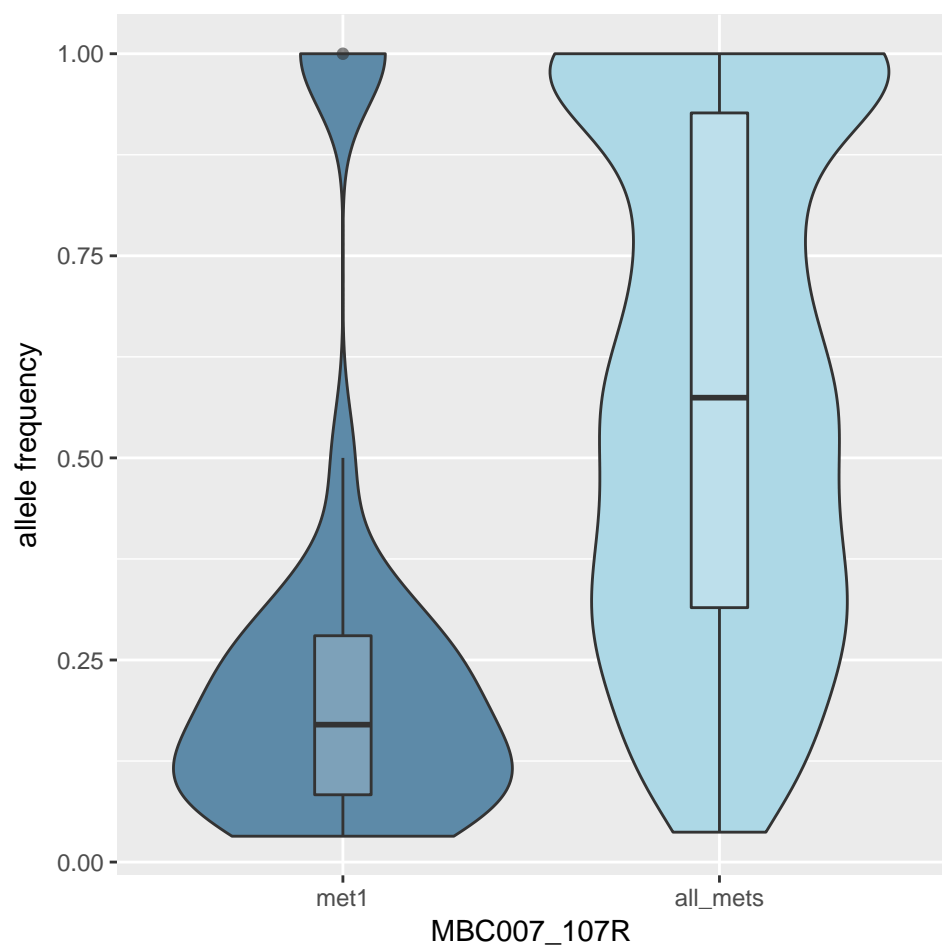




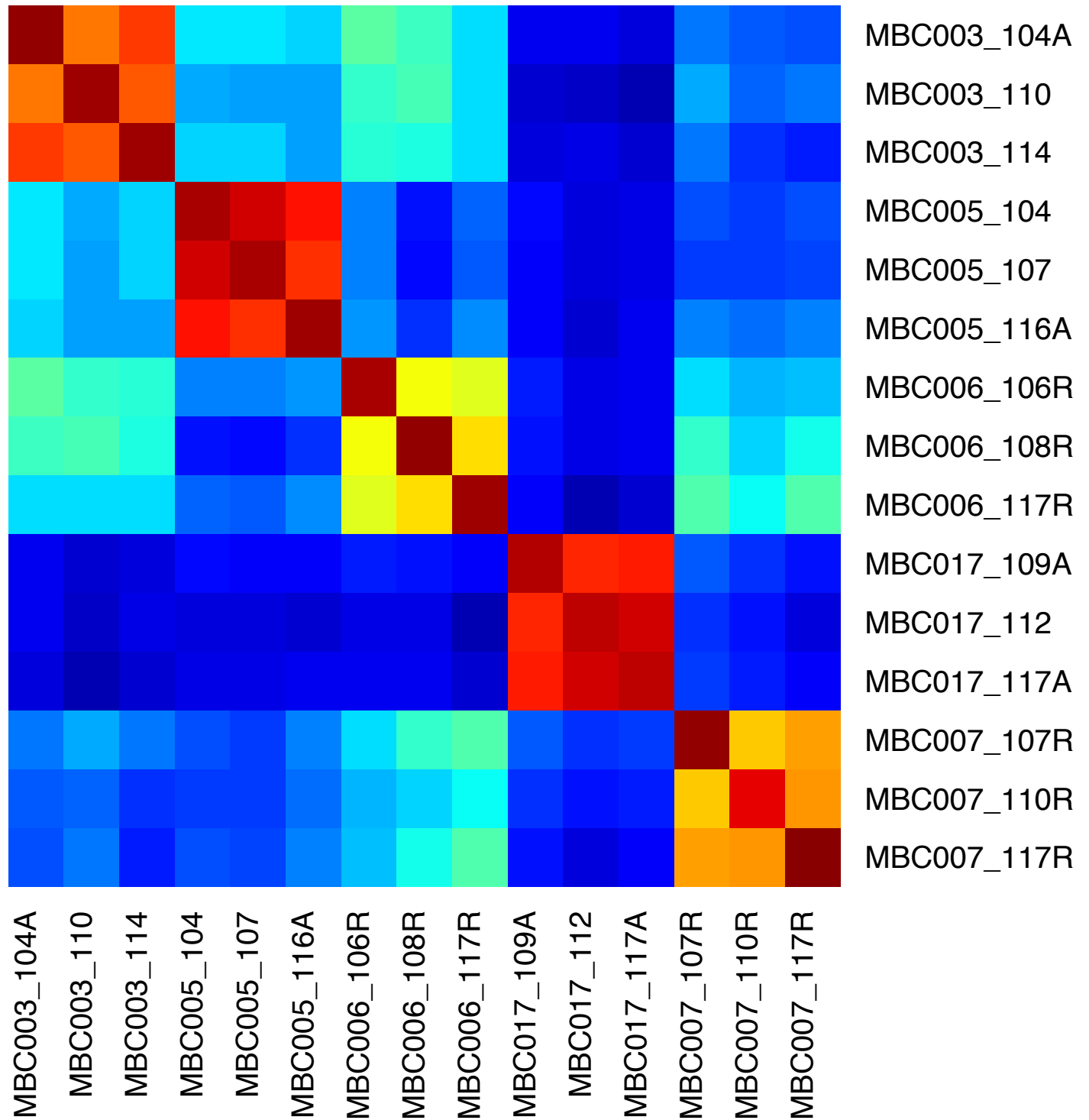
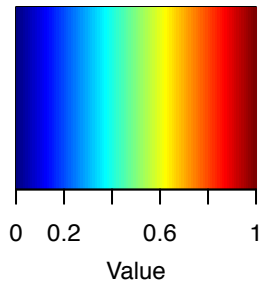




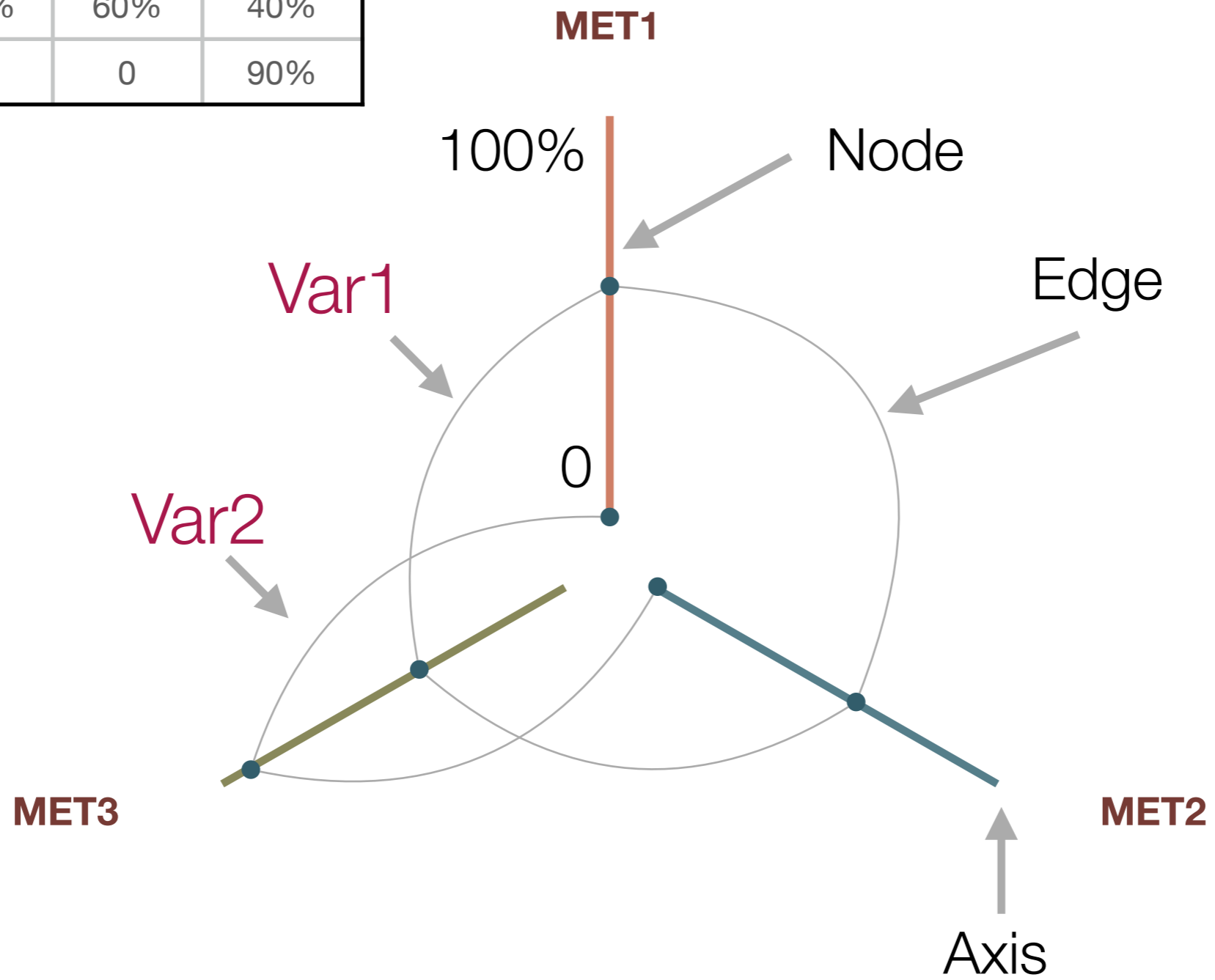




Pearson Correlation Scores Copy Number Variants



Variant	MET1	MET2	MET3
Var1	50%	60%	40%
Var2	0	0	90%



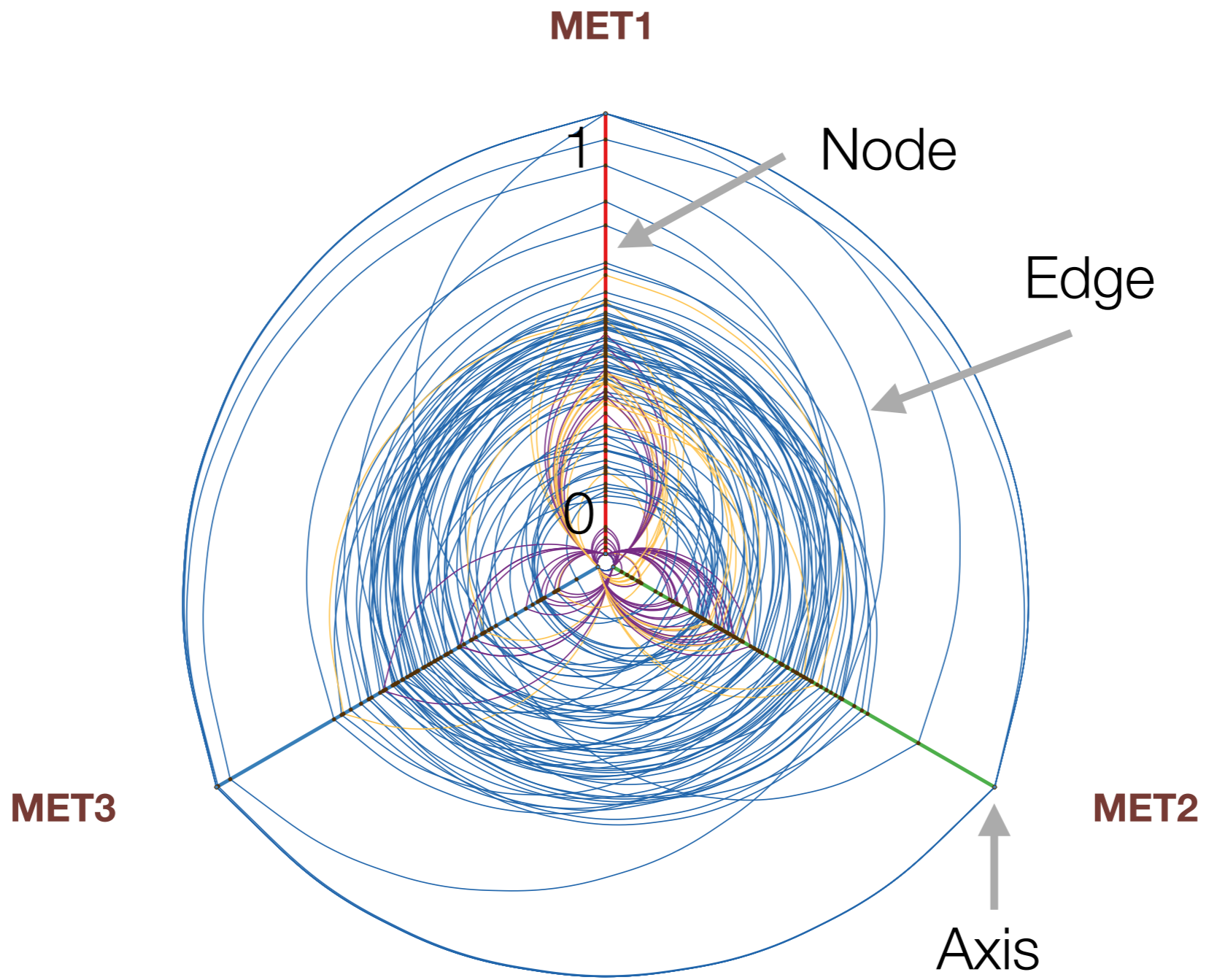


Table S1. Patient sample data

Sample information including average coverage, the fraction of genome altered by copy number and loss of heterozygosity, mutation burden (the number of somatic variants per megabase sequenced), and the anatomical site at which the metastasis was found.

patient	sample	Read Counts	Average coverage	% bases covered by > 1x	fraction genome altered by CNV	fraction genome altered by LOH	# SNVs/Mb sequenced	Organ
MBC003	MBC003_104 A	43,458,282	51.76	99.4	0.3140	0.0745	24.81	Liver
	MBC003_110	54,146,832	63.41	99.75	0.4981	0.2592	24.99	Omentum
	MBC003_114	55,986,876	64.76	99.8	0.3775	0.1581	25.13	Rib
MBC005	MBC005_104	63,577,258	73.15	99.8	0.2740	0.0024	16.47	Liver
	MBC005_107	57,796,398	66.16	99.79	0.2368	0.0206	15.08	Pericardium
	MBC005_116 A	56,122,046	60.64	99.77	0.3692	0.0040	15.94	Pancreas
MBC006	MBC006_106 R	51,384,446	62.94	99.31	0.0296	0.0046	10.86	L Liver
	MBC006_108 R	50,241,694	59.35	99.31	0.2106	0.0141	11.13	Thoracic Spine
	MBC006_117R	57,947,280	68.26	99.35	0.2355	0.0268	11.02	Colon
MBC007	MBC017_109 A	56,267,454	66.80	99.35	0.4584	0.0755	10.04	Omentum
	MBC017_112	59,770,084	71.30	99.31	0.6678	0.4444	9.67	Liver
	MBC017_117 A	52,384,814	58.65	99.14	0.6325	0.4303	9.57	Mediastinal LN
MBC017	MBC007_107 R	57,611,258	67.98	99.81	0.6372	0.3985	11.23	Liver
	MBC007_110R	72,202,640	82.90	99.83	0.4246	0.0182	11.71	Med LN

patient	sample	Read Counts	Average coverage	% bases covered by > 1x	fraction genome altered by CNV	fraction genome altered by LOH	# SNVs/Mb sequenced	Organ
	MBC007_117R	48,802,444	51.76	99.4	0.6129	0.0528	11.19	PeriAo LN

Table S2. Patient Clinical Data

The cases in this study derive from a previously completed rapid autopsy program for patients with metastatic breast cancer. Briefly, patients with terminal metastatic breast cancer consented to have a rapid autopsy performed within a few hours after their death so that metastatic tumors could be harvested for research purpose. The basic clinicopathologic features of the first ten cases in this study, which include the first four cases analyzed in this current study (MBC3, MBC5, MBC6, and MBC7) have previously been described (Wu JM Clinical Cancer Research 2008; 14:1938-1946). Further information is provided below.

MBC003:

This patient was a 40 year old Caucasian female who at age 40 underwent mastectomy for an ER (90%, strong) and PR (20%, weak) positive, HER2 borderline amplified invasive ductal carcinoma, Elston grade 2 of 3. The primary tumor was 2 cm and involved 1 out of 17 axillary lymph nodes (pathologic stage pT1N1). She received chemotherapy (doxorubicin and cytoxan) and took 5 years of tamoxifen. At the end of her course of tamoxifen the patient developed bony metastasis. She did not respond to goserelin for metastatic disease. She succumbed to her metastatic breast carcinoma 2 years later at age 48, with dominant metastases at autopsy involving the liver, lung, brain, omentum, adrenal, spine, and rib. Samples from the left liver, omentum, and rib were analyzed by whole exome sequencing.

MBC005:

This patient was a 59 year old African American female who developed an ER (100%, strong) and PR (20%, weak) positive invasive ductal carcinoma, Elston grade 2 of 3, which was E-cadherin positive and HER2 negative. The primary tumor was 2 cm and node negative (pathologic stage pT1N0). After three years of adjuvant treatment with tamoxifen, the patient developed bony metastasis. She responded well to treatment with aromatase inhibitors (anastrozole) along with pamidronate, but succumbed to her metastatic breast carcinoma 8 years after diagnosis at age 68.

At autopsy, she had extensive disease involving the liver, pancreas, pleura and pericardium, adrenal, bone and brain. Interestingly, as previously described by Wu. et al. (*Clin Cancer Res* 2008), her main metastatic tumor had a lobular phenotype and was negative for E-cadherin by immunohistochemistry. This morphology was present for the majority of the metastases, including liver, pancreas, adrenal, spine and brain, and these metastases were positive for ER (60%, weak) and minimally positive for PR (5%, moderate). Her metastases involving the pericardium and pleural surface of the lung had a predominant ductal phenotype with retained E-cadherin, and were similarly positive for ER (60%, weak), but now strongly immunoreactive for PR (80%, strong). Tumors from the left liver, pancreas and pericardium were analyzed by whole exome sequencing.

Genomic analysis correlated well with the variable phenotype of the metastases. E-cadherin mutations were found in the liver and pancreatic metastasis, but not the pericardial metastasis, consistent with the morphology and E-cadherin immunohistochemistry. Beta-catenin was mutated in all metastases. By immunohistochemistry, beta-catenin was cytoplasmically distributed in pericardium and pleura, and absent in all other metastases. As beta-catenin is typically localized to the cell membrane, the results are consistent with dysfunctional cytoplasmic beta-catenin in the pericardial and pleural metastases, with loss of beta-catenin secondary to E-cadherin inactivation (and resulting destabilization of the E-cadherin/catenin complex) in the other metastases. A mutation in estrogen receptor was identified only within the pericardial metastasis, which correlated with the marked upregulation of p21 and progesterone receptor relative to other metastases.

MBC006:

The patient was a 56 year old Caucasian female who underwent modified radical mastectomy for an ER (80%, strong) and PR (30%, strong) positive, HER2 negative multifocal invasive ductal carcinoma, Elston grade 2 of 3. The breast carcinomas measured 2.8 and 1.7cm and involved two of twenty axillary lymph nodes at diagnosis (pathologic stage pT2N1). The patient received doxorubicin and cytoxan chemotherapy. She initially took anastrozole but did not tolerate it, and switched to tamoxifen. She developed metastases on tamoxifen involving the liver, lung, mediastinal lymph nodes and bone 5 years after diagnosis. She succumbed to her disease one year later at age 61.

At autopsy, her dominant metastases involved the liver, pleura, spine, colon, mediastinal lymph nodes, and epicardium. The metastases were now ER and PR negative, correlating with the clinical loss of hormone responsiveness. Samples from the liver, colon, and spine were analyzed by whole exome sequencing. Of note, while all 3 samples demonstrated a *PIK3CA* mutation, only the spinal metastasis demonstrate a *PTEN* mutation. Of note, this was the only metastasis which demonstrated upregulation of phosphorylated mammalian target of rapamycin (pmTOR), and phosphorylated S6 (pS6) by immunohistochemistry. Correlating with this variability in the mTOR pathway, some but not all of the metastases demonstrated loss by *PTEN* by FISH, whereas this variability was not found on *PTEN* FISH in the other four cases studied.

MBC007:

The patient was a 51 year old female with a history of Hodgkin's disease treated with ABVD chemotherapy and mantle irradiation who developed a triple negative (ER/PR/HER2 negative) invasive ductal carcinoma, Elston grade 3 of 3, and underwent right radical mastectomy. She proved to have a 2 cm high grade invasive ductal carcinoma that was sentinel lymph node negative (pathologic stage pT1N0). She received adjuvant chemotherapy. Two years later, she developed brain metastases and died of disease within one year at age 53. At autopsy, her dominant metastases involved brain, lung, mediastinum, adrenal gland, spine and omentum. Samples from the liver, omentum, and mediastinum were analyzed by whole exome sequencing. Of note, this neoplasm demonstrated a *TP53* mutation in all metastases. This correlated with diffuse immunoreactivity of p53 protein by immunohistochemistry in the primary tumor and all metastases.

MBC017:

The patient was a 47 year old Caucasian female who developed a triple negative (ER/PR/HER2 negative) breast carcinoma, Elston grade 3 of 3, treated by mastectomy. The tumor proved to be 2.3 cm and was node negative though isolated tumor cells were noted (pathologic stage pT2N0 (i+)). The patient received adjuvant chemotherapy but then developed metastases to the lung, liver and bone two years later and died of her disease within one year. At autopsy, her dominant metastases involved, liver, periaortic and mediastinal lymph nodes. Samples from the liver, periaortic lymph nodes and mediastinal lymph nodes were analyzed by whole exome sequencing. Of note, TP53 mutations were identified in all metastases, which correlated with diffuse immunoreactivity for p53 in the primary tumor and all metastases.

Table S3. Copy number variants for commonly altered genes in breast cancer

Sample	Chromosome	Start	End	Gene	Copy Number
MBC003104A	chr17	39688083	39717657	ERBB2	3
MBC003_110	chr17	39688083	39717657	ERBB2	3
MBC003_114	chr17	39688083	39717657	ERBB2	3
MBC005_104	chr17	39688083	39717657	ERBB2	2
MBC005_107	chr17	39688083	39717657	ERBB2	2
MBC005_116A	chr17	39688083	39717657	ERBB2	1
MBC006_106R	chr17	39688083	39717657	ERBB2	2
MBC006_108R	chr17	39688083	39717657	ERBB2	2
MBC006_117R	chr17	39688083	39717657	ERBB2	1
MBC007_107R	chr17	39688083	39717657	ERBB2	1
MBC007_110R	chr17	39688083	39717657	ERBB2	3
MBC007_117R	chr17	39688083	39717657	ERBB2	3
MBC017_109A	chr17	39688083	39717657	ERBB2	2
MBC017_112	chr17	39688083	39717657	ERBB2	2
MBC017_117A	chr17	39688083	39717657	ERBB2	1
MBC003_104A	chr8	80034869	80080831	TPD52	8
MBC003_110	chr8	80034869	80080831	TPD52	13
MBC003_114	chr8	80034869	80080831	TPD52	15
MBC005_104	chr8	80034869	80080831	TPD52	3
MBC005_107	chr8	80034869	80080831	TPD52	3
MBC005_116A	chr8	80034869	80080831	TPD52	3
MBC006_106R	chr8	80034869	80080831	TPD52	4
MBC006_108R	chr8	80034869	80080831	TPD52	8
MBC006_117R	chr8	80034869	80080831	TPD52	8
MBC007_107R	chr8	80034869	80080831	TPD52	4
MBC007_110R	chr8	80034869	80080831	TPD52	3
MBC007_117R	chr8	80034869	80080831	TPD52	4
MBC017_109A	chr8	80034869	80080831	TPD52	3
MBC017_112	chr8	80034869	80080831	TPD52	3
MBC017_117A	chr8	80034869	80080831	TPD52	3

MBC003_104A	chr10	121478329	121596645	FGFR2	2
MBC003_110	chr10	121478329	121596645	FGFR2	1
MBC003_114	chr10	121478329	121596645	FGFR2	2
MBC005_104	chr10	121478329	121596645	FGFR2	2
MBC005_107	chr10	121478329	121596645	FGFR2	2
MBC005_116A	chr10	121478329	121596645	FGFR2	2
MBC006_106R	chr10	121478329	121596645	FGFR2	2
MBC006_108R	chr10	121478329	121596645	FGFR2	2
MBC006_117R	chr10	121478329	121596645	FGFR2	2
MBC007_107R	chr10	121478329	121596645	FGFR2	3
MBC007_110R	chr10	121478329	121596645	FGFR2	2
MBC007_117R	chr10	121478329	121596645	FGFR2	1
MBC017_109A	chr10	121478329	121596645	FGFR2	62
MBC017_112	chr10	121478329	121596645	FGFR2	78
MBC017_117A	chr10	121478329	121596645	FGFR2	71
MBC003_104A	chr19	15159632	15200981	NOTCH3	2
MBC003_110	chr19	15159632	15200981	NOTCH3	1
MBC003_114	chr19	15159632	15200981	NOTCH3	2
MBC005_104	chr19	15159632	15200981	NOTCH3	2
MBC005_107	chr19	15159632	15200981	NOTCH3	2
MBC005_116A	chr19	15159632	15200981	NOTCH3	1
MBC006_106R	chr19	15159632	15200981	NOTCH3	2
MBC006_108R	chr19	15159632	15200981	NOTCH3	2
MBC006_117R	chr19	15159632	15200981	NOTCH3	2
MBC007_107R	chr19	15159632	15200981	NOTCH3	1
MBC007_110R	chr19	15159632	15200981	NOTCH3	1
MBC007_117R	chr19	15159632	15200981	NOTCH3	1
MBC017_109A	chr19	15159632	15200981	NOTCH3	2
MBC017_112	chr19	15159632	15200981	NOTCH3	2
MBC017_117A	chr19	15159632	15200981	NOTCH3	2
MBC003_104A	chr9	21967751	21975133	CDKN2A	2
MBC003_110	chr9	21967751	21975133	CDKN2A	1
MBC003_114	chr9	21967751	21975133	CDKN2A	2

MBC005_104	chr9	21967751	21975133	CDKN2A	1
MBC005_107	chr9	21967751	21975133	CDKN2A	2
MBC005_116A	chr9	21967751	21975133	CDKN2A	1
MBC006_106R	chr9	21967751	21975133	CDKN2A	2
MBC006_108R	chr9	21967751	21975133	CDKN2A	1
MBC006_117R	chr9	21967751	21975133	CDKN2A	1
MBC007_107R	chr9	21967751	21975133	CDKN2A	2
MBC007_110R	chr9	21967751	21975133	CDKN2A	4
MBC007_117R	chr9	21967751	21975133	CDKN2A	3
MBC017_109A	chr9	21967751	21975133	CDKN2A	1
MBC017_112	chr9	21967751	21975133	CDKN2A	1
MBC017_117A	chr9	21967751	21975133	CDKN2A	1
MBC003_104A	chr17	40388520	40417950	TOP2A	3
MBC003_110	chr17	40388520	40417950	TOP2A	3
MBC003_114	chr17	40388520	40417950	TOP2A	3
MBC005_104	chr17	40388520	40417950	TOP2A	2
MBC005_107	chr17	40388520	40417950	TOP2A	2
MBC005_116A	chr17	40388520	40417950	TOP2A	1
MBC006_106R	chr17	40388520	40417950	TOP2A	2
MBC006_108R	chr17	40388520	40417950	TOP2A	2
MBC006_117R	chr17	40388520	40417950	TOP2A	1
MBC007_107R	chr17	40388520	40417950	TOP2A	1
MBC007_110R	chr17	40388520	40417950	TOP2A	1
MBC007_117R	chr17	40388520	40417950	TOP2A	1
MBC017_109A	chr17	40388520	40417950	TOP2A	2
MBC017_112	chr17	40388520	40417950	TOP2A	2
MBC017_117A	chr17	40388520	40417950	TOP2A	1
MBC003_104A	chr8	103298830	103332866	FZD6	6
MBC003_110	chr8	103298830	103332866	FZD6	10
MBC003_114	chr8	103298830	103332866	FZD6	8
MBC005_104	chr8	103298830	103332866	FZD6	3
MBC005_107	chr8	103298830	103332866	FZD6	3
MBC005_116A	chr8	103298830	103332866	FZD6	3

MBC006_106R	chr8	103298830	103332866	FZD6	2
MBC006_108R	chr8	103298830	103332866	FZD6	2
MBC006_108R	chr8	103298830	103332866	FZD6	3
MBC006_117R	chr8	103298830	103332866	FZD6	2
MBC007_107R	chr8	103298830	103332866	FZD6	4
MBC007_110R	chr8	103298830	103332866	FZD6	3
MBC007_117R	chr8	103298830	103332866	FZD6	4
MBC017_109A	chr8	103298830	103332866	FZD6	3
MBC017_112	chr8	103298830	103332866	FZD6	3
MBC017_117A	chr8	103298830	103332866	FZD6	3
MBC003_104A	chr17	39200282	39204727	RPL19	1
MBC003_110	chr17	39200282	39204727	RPL19	1
MBC003_114	chr17	39200282	39204727	RPL19	1
MBC005_104	chr17	39200282	39204727	RPL19	2
MBC005_107	chr17	39200282	39204727	RPL19	2
MBC005_116A	chr17	39200282	39204727	RPL19	1
MBC006_106R	chr17	39200282	39204727	RPL19	2
MBC006_108R	chr17	39200282	39204727	RPL19	2
MBC006_117R	chr17	39200282	39204727	RPL19	1
MBC007_107R	chr17	39200282	39204727	RPL19	1
MBC007_110R	chr17	39200282	39204727	RPL19	1
MBC007_117R	chr17	39200282	39204727	RPL19	1
MBC017_109A	chr17	39200282	39204727	RPL19	2
MBC017_112	chr17	39200282	39204727	RPL19	2
MBC017_117A	chr17	39200282	39204727	RPL19	1
MBC003_104A	chr8	38411137	38468834	FGFR1	3
MBC003_110	chr8	38411137	38468834	FGFR1	5
MBC003_114	chr8	38411137	38468834	FGFR1	3
MBC005_104	chr8	38411137	38468834	FGFR1	3
MBC005_107	chr8	38411137	38468834	FGFR1	3
MBC005_116A	chr8	38411137	38468834	FGFR1	3
MBC006_106R	chr8	38411137	38468834	FGFR1	3
MBC006_108R	chr8	38411137	38468834	FGFR1	5

MBC006_117R	chr8	38411137	38468834	FGFR1	11
MBC007_107R	chr8	38411137	38468834	FGFR1	9
MBC007_110R	chr8	38411137	38468834	FGFR1	8
MBC007_117R	chr8	38411137	38468834	FGFR1	13
MBC017_109A	chr8	38411137	38468834	FGFR1	2
MBC017_112	chr8	38411137	38468834	FGFR1	1
MBC017_117A	chr8	38411137	38468834	FGFR1	1
MBC003_104A	chr8	127736068	127741434	MYC	8
MBC003_110	chr8	127736068	127741434	MYC	8
MBC003_114	chr8	127736068	127741434	MYC	9
MBC005_104	chr8	127736068	127741434	MYC	3
MBC005_107	chr8	127736068	127741434	MYC	3
MBC005_116A	chr8	127736068	127741434	MYC	3
MBC006_106R	chr8	127736068	127741434	MYC	3
MBC006_108R	chr8	127736068	127741434	MYC	4
MBC006_117R	chr8	127736068	127741434	MYC	5
MBC007_107R	chr8	127736068	127741434	MYC	4
MBC007_110R	chr8	127736068	127741434	MYC	3
MBC007_117R	chr8	127736068	127741434	MYC	4
MBC017_109A	chr8	127736068	127741434	MYC	3
MBC017_112	chr8	127736068	127741434	MYC	3
MBC017_117A	chr8	127736068	127741434	MYC	3
MBC003_104A	chr15	51208056	51338598	CYP19A1	1
MBC003_110	chr15	51208056	51338598	CYP19A1	1
MBC003_114	chr15	51208056	51338598	CYP19A1	1
MBC005_104	chr15	51208056	51338598	CYP19A1	2
MBC005_107	chr15	51208056	51338598	CYP19A1	2
MBC005_116A	chr15	51208056	51338598	CYP19A1	2
MBC006_106R	chr15	51208056	51338598	CYP19A1	2
MBC006_108R	chr15	51208056	51338598	CYP19A1	2
MBC006_117R	chr15	51208056	51338598	CYP19A1	2
MBC007_107R	chr15	51208056	51338598	CYP19A1	1
MBC007_110R	chr15	51208056	51338598	CYP19A1	1

MBC007_117R	chr15	51208056	51338598	CYP19A1	1
MBC017_109A	chr15	51208056	51338598	CYP19A1	2
MBC017_112	chr15	51208056	51338598	CYP19A1	3
MBC017_117A	chr15	51208056	51338598	CYP19A1	3
MBC003_104A	chr19	29811993	29824317	CCNE1	2
MBC003_110	chr19	29811993	29824317	CCNE1	2
MBC003_114	chr19	29811993	29824317	CCNE1	2
MBC005_104	chr19	29811993	29824317	CCNE1	2
MBC005_107	chr19	29811993	29824317	CCNE1	2
MBC005_116A	chr19	29811993	29824317	CCNE1	1
MBC006_106R	chr19	29811993	29824317	CCNE1	2
MBC006_108R	chr19	29811993	29824317	CCNE1	2
MBC006_117R	chr19	29811993	29824317	CCNE1	2
MBC007_107R	chr19	29811993	29824317	CCNE1	6
MBC007_107R	chr19	29811993	29824317	CCNE1	8
MBC007_110R	chr19	29811993	29824317	CCNE1	6
MBC007_117R	chr19	29811993	29824317	CCNE1	9
MBC017_109A	chr19	29811993	29824317	CCNE1	2
MBC017_112	chr19	29811993	29824317	CCNE1	2
MBC017_117A	chr19	29811993	29824317	CCNE1	2
MBC003_104A	chr11	108222831	108369099	ATM	1
MBC003_110	chr11	108222831	108369099	ATM	1
MBC003_114	chr11	108222831	108369099	ATM	1
MBC005_104	chr11	108222831	108369099	ATM	1
MBC005_107	chr11	108222831	108369099	ATM	1
MBC005_116A	chr11	108222831	108369099	ATM	1
MBC006_106R	chr11	108222831	108369099	ATM	2
MBC006_108R	chr11	108222831	108369099	ATM	2
MBC006_117R	chr11	108222831	108369099	ATM	2
MBC007_107R	chr11	108222831	108369099	ATM	2
MBC007_110R	chr11	108222831	108369099	ATM	2
MBC007_117R	chr11	108222831	108369099	ATM	2
MBC017_109A	chr11	108222831	108369099	ATM	1

MBC017_112	chr11	108222831	108369099	ATM	2
MBC017_117A	chr11	108222831	108369099	ATM	1
MBC003_104A	chr10	87863437	87971930	PTEN	2
MBC003_110	chr10	87863437	87971930	PTEN	2
MBC003_114	chr10	87863437	87971930	PTEN	2
MBC005_104	chr10	87863437	87971930	PTEN	2
MBC005_107	chr10	87863437	87971930	PTEN	2
MBC005_116A	chr10	87863437	87971930	PTEN	2
MBC006_106R	chr10	87863437	87971930	PTEN	2
MBC006_108R	chr10	87863437	87971930	PTEN	2
MBC006_117R	chr10	87863437	87971930	PTEN	2
MBC007_107R	chr10	87863437	87971930	PTEN	1
MBC007_110R	chr10	87863437	87971930	PTEN	2
MBC007_117R	chr10	87863437	87971930	PTEN	1
MBC017_109A	chr10	87863437	87971930	PTEN	1
MBC017_112	chr10	87863437	87971930	PTEN	1
MBC017_117A	chr10	87863437	87971930	PTEN	1
MBC003_104A	chr14	37589551	37595120	FOXA1	4
MBC003_110	chr14	37589551	37595120	FOXA1	6
MBC003_114	chr14	37589551	37595120	FOXA1	4
MBC005_104	chr14	37589551	37595120	FOXA1	2
MBC005_107	chr14	37589551	37595120	FOXA1	2
MBC005_116A	chr14	37589551	37595120	FOXA1	2
MBC006_106R	chr14	37589551	37595120	FOXA1	2
MBC006_108R	chr14	37589551	37595120	FOXA1	2
MBC006_117R	chr14	37589551	37595120	FOXA1	2
MBC007_107R	chr14	37589551	37595120	FOXA1	1
MBC007_110R	chr14	37589551	37595120	FOXA1	1
MBC007_117R	chr14	37589551	37595120	FOXA1	1
MBC017_109A	chr14	37589551	37595120	FOXA1	1
MBC017_112	chr14	37589551	37595120	FOXA1	1
MBC017_117A	chr14	37589551	37595120	FOXA1	1
MBC003_104A	chr12	4273735	4305356	CCND2	2

MBC003_110	chr12	4273735	4305356	CCND2	1
MBC003_114	chr12	4273735	4305356	CCND2	2
MBC005_104	chr12	4273735	4305356	CCND2	2
MBC005_107	chr12	4273735	4305356	CCND2	2
MBC005_116A	chr12	4273735	4305356	CCND2	2
MBC006_106R	chr12	4273735	4305356	CCND2	2
MBC006_108R	chr12	4273735	4305356	CCND2	2
MBC006_117R	chr12	4273735	4305356	CCND2	2
MBC007_107R	chr12	4273735	4305356	CCND2	2
MBC007_110R	chr12	4273735	4305356	CCND2	2
MBC007_117R	chr12	4273735	4305356	CCND2	2
MBC017_109A	chr12	4273735	4305356	CCND2	3
MBC017_112	chr12	4273735	4305356	CCND2	3
MBC017_117A	chr12	4273735	4305356	CCND2	3
MBC003_104A	chr11	68707439	68751520	TESMIN	5
MBC003_110	chr11	68707439	68751520	TESMIN	5
MBC003_114	chr11	68707439	68751520	TESMIN	5
MBC005_104	chr11	68707439	68751520	TESMIN	2
MBC005_107	chr11	68707439	68751520	TESMIN	2
MBC005_116A	chr11	68707439	68751520	TESMIN	2
MBC006_106R	chr11	68707439	68751520	TESMIN	2
MBC006_108R	chr11	68707439	68751520	TESMIN	2
MBC006_117R	chr11	68707439	68751520	TESMIN	2
MBC007_107R	chr11	68707439	68751520	TESMIN	2
MBC007_110R	chr11	68707439	68751520	TESMIN	2
MBC007_117R	chr11	68707439	68751520	TESMIN	2
MBC017_109A	chr11	68707439	68751520	TESMIN	3
MBC017_112	chr11	68707439	68751520	TESMIN	3
MBC017_117A	chr11	68707439	68751520	TESMIN	3
MBC003_104A	chr8	144511283	144517826	RECQL4	2
MBC003_110	chr8	144511283	144517826	RECQL4	1
MBC003_114	chr8	144511283	144517826	RECQL4	1
MBC005_104	chr8	144511283	144517826	RECQL4	3

MBC005_107	chr8	144511283	144517826	RECQL4	3
MBC005_116A	chr8	144511283	144517826	RECQL4	2
MBC006_106R	chr8	144511283	144517826	RECQL4	1
MBC006_108R	chr8	144511283	144517826	RECQL4	1
MBC006_117R	chr8	144511283	144517826	RECQL4	1
MBC007_107R	chr8	144511283	144517826	RECQL4	3
MBC007_110R	chr8	144511283	144517826	RECQL4	3
MBC007_117R	chr8	144511283	144517826	RECQL4	4
MBC017_109A	chr8	144511283	144517826	RECQL4	3
MBC017_112	chr8	144511283	144517826	RECQL4	5
MBC017_117A	chr8	144511283	144517826	RECQL4	4
MBC003_104A	chr7	116672358	116798386	MET	2
MBC003_110	chr7	116672358	116798386	MET	2
MBC003_114	chr7	116672358	116798386	MET	2
MBC005_104	chr7	116672358	116798386	MET	1
MBC005_107	chr7	116672358	116798386	MET	1
MBC005_116A	chr7	116672358	116798386	MET	1
MBC006_106R	chr7	116672358	116798386	MET	2
MBC006_108R	chr7	116672358	116798386	MET	2
MBC006_117R	chr7	116672358	116798386	MET	3
MBC007_107R	chr7	116672358	116798386	MET	3
MBC007_110R	chr7	116672358	116798386	MET	2
MBC007_117R	chr7	116672358	116798386	MET	2
MBC017_109A	chr7	116672358	116798386	MET	2
MBC017_112	chr7	116672358	116798386	MET	2
MBC017_117A	chr7	116672358	116798386	MET	2
MBC003_104A	chr3	25597904	25664499	TOP2B	3
MBC003_110	chr3	25597904	25664499	TOP2B	4
MBC003_114	chr3	25597904	25664499	TOP2B	4
MBC005_104	chr3	25597904	25664499	TOP2B	2
MBC005_107	chr3	25597904	25664499	TOP2B	2
MBC005_116A	chr3	25597904	25664499	TOP2B	2
MBC006_106R	chr3	25597904	25664499	TOP2B	2

MBC006_108R	chr3	25597904	25664499	TOP2B	2
MBC006_117R	chr3	25597904	25664499	TOP2B	2
MBC007_107R	chr3	25597904	25664499	TOP2B	1
MBC007_110R	chr3	25597904	25664499	TOP2B	1
MBC007_117R	chr3	25597904	25664499	TOP2B	1
MBC017_109A	chr3	25597904	25664499	TOP2B	1
MBC017_112	chr3	25597904	25664499	TOP2B	1
MBC017_117A	chr3	25597904	25664499	TOP2B	1

Table S4. Genetic similarity scores

Genetic similarity scores for each metastatic tumor in the High, Moderate and Low impact categories and for all categories collectively. The score is computed as $\frac{\# \text{ shared variants}}{\# \text{ shared variants} + (\# \text{ unique variants} / 2)}$, where shared variants are those that are found in all metastases from the patient.

Patient	Tumor Pair	valid	high	moderate	low	dbSNP
MBC005	MBC005_104-MBC005_107	0.93	0.67	0.77	0.92	0.99
	MBC005_104-MBC005_116A	0.94	0.67	0.84	0.92	0.99
	MBC005_107-MBC005_116A	0.93	0.57	0.76	0.91	0.99
MBC006	MBC006_106R-MBC006_108R	0.90	0.47	0.84	0.89	0.99
	MBC006_106R-MBC006_117R	0.90	0.47	0.83	0.89	0.99
	MBC006_108R-MBC006_117R	0.91	0.56	0.85	0.90	1.00
MBC003	MBC003_104A-MBC003_110	0.93	0.77	0.88	0.94	0.99
	MBC003_104A-MBC003_114	0.93	0.77	0.88	0.94	0.99

	MBC003_110-MBC003_114	0.93	0.77	0.89	0.94	0.99
MBC007	MBC007_107R-MBC007_110R	0.92	0.67	0.85	0.95	0.98
	MBC007_107R-MBC007_117R	0.91	0.67	0.84	0.94	0.97
	MBC007_110R-MBC007_117R	0.92	0.67	0.85	0.95	0.99
MBC017	MBC017_109A-MBC017_112	0.93	1.00	0.95	0.94	0.96
	MBC017_109A-MBC017_117A	0.94	1.00	0.96	0.95	0.98
	MBC017_112-MBC017_117A	0.93	1.00	0.93	0.95	0.95

Supplemental Figures

Figure S1. Data analysis workflow

Data analysis workflow, including alignment and somatic variant calling.

Figure S2. *TP53* mutation in samples from patient MBC007

Diffuse immunoreactivity for p53 correlates with consistent p53 mutations in all metastases (MBC007). In this case, all metastases demonstrated the same *TP53* mutation. Diffuse p53 immunoreactivity was identified by immunohistochemistry in the primary tumor and in all metastases. (A) Tissue microarray (40x) demonstrating four spots including liver (upper) and bony (lower) metastases. (B) Low power view (40x) of p53 immunoreactivity in these metastases, highlighting diffuse immunoreactivity. (C) High power view (400x) of bony metastases, demonstrating high grade morphology typical of a triple negative breast carcinoma. (D) High power immunohistochemistry (400x) of bony metastasis p53 immunostaining, demonstrating diffuse nuclear labeling of neoplastic cells and absence of labeling in endothelial cells.

Figure S3. *PTEN* mutation in patient MBC006

Variable upregulation of mammalian target of rapamycin (mTOR) signaling correlates with variable *PTEN* mutation in metastases (MBC006). This patient's spinal metastases demonstrated a *PTEN* mutation, which was not found in the liver or colon metastases. By immunohistochemistry, this patient's spinal metastasis (A) demonstrated immunohistochemical labeling for phosphorylated mTOR (pmTOR) (B), and phosphorylated S6 (pS6), (C) which reflects active upregulated mTOR signaling. In contrast, all of the other metastases in this case found on patient specific tissue microarray including the liver metastases (D) did not demonstrated labeling for either pmTOR (E), (note intact labeling of entrapped bile ducts serving as an internal control) or pS6 (F). All images 400x magnification.

Figure S4. Detailed allele frequency, CNV, and LOH in circle plots (A) and hive plots (B) for all samples

Figure S5. Violin plots depicting allele distribution for shared and private variants in all metastases.

Figure S6. Pearson correlation coefficients for copy number alterations

Figure S7. Explanation of hive plot layout

We provide a short demonstration to assist in interpreting the hive plots.

Supplemental Tables

Table S1.

Sample information including average coverage, the fraction of genome altered by copy number and loss of heterozygosity, mutation burden (the number of somatic variants per megabase sequenced), and the anatomical site at which the metastasis was found.

Table S2. Case histories for 5 patients.

Table S3. Allele frequencies for commonly mutated genes in breast cancer

Table S4. Copy number variants spanning commonly altered genes in breast cancer

Table S5. Genetic similarity scores for each metastatic tumor in the high, moderate and low impact categories and for all categories collectively. The score is computed as $\# \text{ shared variants} / (\# \text{ shared variants} + (\# \text{ unique variants} / 2))$, where shared variants are those that are found in all metastases from the patient.

Supplemental Data

Somatic variant calls for each of the 5 sets of metastases are provided in vcf text files as supplemental data. Two files for each patient give allele frequencies and further information for all three metastases, one file for all valid calls and another that includes all valid calls and those mutations that were found in COSMIC and the panel of normals.